Recent Progresses in Mid Infrared Nanocrystal based Optoelectronics

Emmanuel Lhuillier, Philippe Guyot-Sionnest

Recent Progresses in Mid Infrared Nanocrystal Optoelectronics

Emmanuel Lhuillier, Philippe Guyot-Sionnest

***Abstract*— Over the past few years, colloidal nanoparticles have started to be investigated for their optical properties in the mid-infrared, past 3 microns. Research on detector application has led to background limited detection and fast video imaging at 5 microns. With further development, one could imagine that these new materials could vastly reduce the costs of infrared technology and this would lead to a trove of new applications for infrared imaging into our daily lives. This article reviews the progress regarding the optical, transport and photodetection properties of thin film based on these materials, and the three different ways by which infrared resonances have been realized with colloidal nanoparticles: interband absorption with small gap semiconductor quantum dots, intraband absorption in lightly doped quantum dots, and plasmonic resonances in heavily doped nanocrystals.**

***Index Terms*— Colloidal quantum dot, infrared, HgTe, HgSe, self-doping, photoresponse.**

I. Introduction

In the mid infrared (λ>3μm) the thermal emission of a room temperature object typically prevails over the reflection of a warm source. The mid-wave infrared (MWIR) between 3 and 5 μm is an eye-safe region and an atmospheric transparency window. The long-wave infrared (LWIR) between 8 and 12μm is where the peak of the 300K blackbody radiation coincides with another atmosphere transmission window. Both ranges are of interest for long distance thermal imaging.

There are two main types of infrared detectors, quantum detectors (sensitive to photon) and thermal detector (sensitive to energy). Quantum detectors operate like visible photodetectors but require small energy gaps and this is challenging from a material perspective. The dominant narrow band gap semiconductors are InSb for the MWIR, as well as $Hg_{1-x}Cd_xTe$ (MCT) which is tunable from MWIR to LWIR by adjusting the composition. To achieve high performance, the materials need to be single crystals with minimal defects and dislocations. On a commercial scale, this is achieved by epitaxial growth on lattice matched substrates by molecular beam epitaxy or chemical vapor deposition, and this leads to high costs. Over the past twenty years, heterostructured wide band gap semiconductors have been developed using superlattices. The infrared absorption is created using intersubband transitions within one of the wells of the superlattice (GaAs/AlGaAs) and these are called Quantum Well Infrared Photodetectors (QWIP) [1] or Type II transitions across wells of the different materials, (InAs/GaSb), called T2SL (Type II Super Lattice) or SLS (Strained Layer Super-lattice). Research on Quantum Dot Infrared Detectors (QDIP) based on self-assembled epitaxial quantum dots also started about twenty years ago [2-6]. QDIPs, while initially very promising, have suffered from limited size control and the low density of the epitaxial quantum dots. Today the dominant commercial quantum detectors are still based on InSb and MCT [7]. The quantum detector technologies aim for high performance applications with high detectivity and high speed. However, the detectors are costly and, combined with the requirement for cooling, their use is largely restricted to defense and research such as high definition camera for astronomy imaging and spectroscopy.

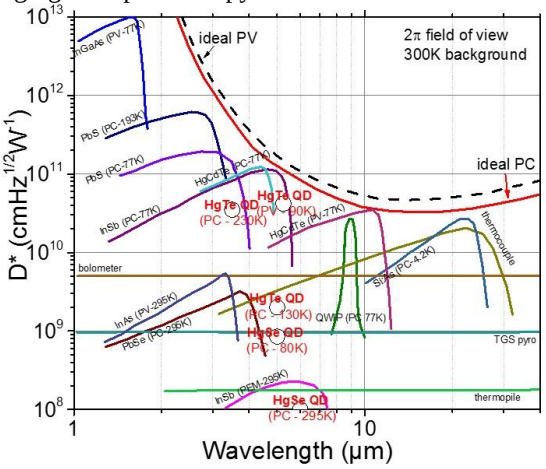

Figure 1 Detectivity as a function of wavelength for different detector technologies. The circles highlight results obtained with HgTe and HgSe CQD, adapted from ref [8]. PC and PV are respectively used for photoconductor and photovoltaic.

Bolometer detection is the leading room temperature technology combining low NETD (30-50mK) with operation at 300K. Bolometers are widely used for cheap thermal motion sensors, and bolometer cameras are leading the market for consumer IR imaging. Two disadvantages of bolometers are an inherently slow time constant of a few ms, and an intrinsically lower detectivity than quantum detectors, especially in the

Manuscript received november 24, 2016. EL acknowledges support from Agence Nationale de la Recherche through grant Nanodose, from the Region Ile-de-France in the framework of DIM Nano-K, from ANR within the Investissements d'Avenir programme ANR-11-IDEX-0004-02, and within the framework of the Cluster of Excellence MATISSE. PGS acknowledges support from ARO W911NF-15-1-1-0110 and from Sivananthan Laboratories, Inc., through an SBIR grant.

EL is with the Sorbonne Universités, UPMC Univ Paris 06, CNRS-UMR 7588, Institut des NanoSciences de Paris, 4 place jussieu, 75005 Paris, France: +33 1 44 27 82 37; el@insp.upmc.fr.

PGS. Author, James Franck Institute, 929 East 57th Street, Chicago, Illinois 60637, USA, pgs@uchiacgo.edu.

MWIR. Figure 1 shows the specific detectivity achieved with various detector technologies.

Since the previous technologies are not likely to lead to a price disruption, an alternative may come from solution processing. Organic electronic which is often seen as the low cost alternative to silicon electronic is ineffective in the mid infrared but inorganic colloidal quantum dots (CQD) are a potential alternative. For the last 30 years, CQDs attracted scientific interest because of their captivating size tunable optical features and because of the ease of fabrication. The first mass market for these nanoparticles appeared a couple year ago as they started to be used as phosphors for TV display [9].

Most of the earlier efforts focused on wide band gap material such as cadmium chalcogenides, Cd(S,Se,Te), with bright visible fluorescence. The lead chalcogenides CQDs, primarily Pb(S,Se), brought the materials to the near-IR with promising developments as optical detector and solar photovoltaic. HgTe CQDs opened the mid-infrared spectral range with photoluminescence and photodetection [10-12].

One may also use the intraband transition of CQDs which removes the need for a small bulk bandgap and widely expands the range of possible IR CQDs. This strategy has so far been demonstrated for HgS and HgSe. In parallel, there has been much interest in semiconductor nanocrystal that exhibit plasmonic resonances, tunable in the mid-IR with the control of the carrier density. These might also become part of future IR technology.

II. NANOCRYSTALS WITH INFRARED PROPERTIES

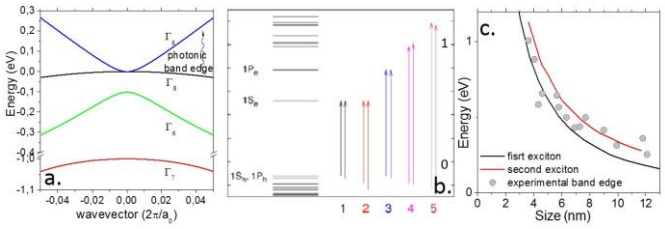

Figure 2a. band structure of bulk HgTe. b. discrete spectrum of HgTe CQD calculated by a tight binding method, adapted from ref [13]. c. Energy of the HgTe interband absorption edge as a function of the nanoparticle size (diameter), adapted from ref [14].

A. *HgTe interband CQDs*

The leading material for mid-IR CQDs is currently HgTe. It is a zero gap semiconductor, also called a semimetal, and any absorption edge can a priori be obtained with quantum confinement. There is a small number of other semimetals, including C (graphene), Bi, Sb, and binary materials, HgSe, Cd_3As_2. There are also very small gap semiconductors such as SnTe, Bi_2Te_3 or Ag_2Te which have been made as nanocrystals. The ternary materials, HgCdTe and PbSnTe, show a zero gap over a range of compositions and InAsSb has a small gap. These materials could be potential alternatives to the HgTe.

Figure 2a shows the k.p band structure for HgTe. The Γ_6 band which has generally the symmetry of a conduction band (in CdTe for example) is below the Γ_8 bands which usually have the valence band symmetry. This inversion of the band is responsible for the "negative value" of the band gap reported for HgTe and HgSe. When HgTe is intrinsic, the Fermi level lies where the two Γ_8 bands meet. The weakly dispersive heavy-hole band with Γ_8 symmetry plays the role of the valence band, while the conduction band is the upper Γ_8 band. The lowest energy interband transition in CQDs occur between the quantum confined states from these two Γ_8 bands. Calculation of the electronic structure of HgTe CQD using a tight binding method (see Figure 2b) have shown a good correlation with experimental results [*13*,14].

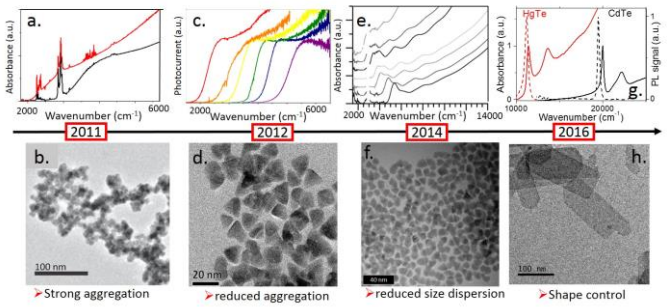

Figure 3 a. absorption spectra of HgTe quantum dots of two sizes, adapted from [21]. b TEM image of the material associated with the spectra of part a. This early synthesis was reaching the 3-5µm range, but the band edge was poorly defined and the material was strongly aggregated. c. Photocurrent spectra of HgTe quantum dots of different sizes, adapted from ref [22]. d TEM image of the material associated with the spectra of part b. This material presents shaper band edge and reduced aggregation. e. Absorption spectra of HgTe quantum dots of several sizes, adapted from ref [13]. f. TEM image of the material associated with the spectra of part c..g Absorption spectra of CdTe and HgTe nanoplatelets, adapted from ref [26]. h. TEM image of the material associated with the spectrum of part g.

For the historical development of the HgTe nanocrystals, the reader is referred to an extensive review of the synthesis of small gap chalcogenide nanoparticles [10]. Briefly, the colloidal synthesis of HgX compounds started with aqueous precipitation [15-17] and evolved towards organometallic methods [18-20] striving for increasingly better control of size and optical properties. The initial small nanocrystals of Hg(Cd)Te had optical absorption and bright luminescence in the near infrared and the interest was to apply the materials for near-IR biolabelling and optoelectronics around the telecom wavelength. In 2011, Keuleyan *et al* [21] developed an HgTe CQD synthesis to obtain optical absorption in the 3-5µm range, specifically for mid-infrared detection. These HgTe CQDs had an absorption tail into the mid-IR and allowed the first photodetection of mid-infrared light with CQDs. However, they showed no resolved excitonic feature, see Figure 3a, and were highly aggregated, see Figure 3b. Improvements of the synthesis led to better resolved features [22] and improved detection properties. A typical synthesis starts with $HgCl_2$ in an oleylamine solvent. At a particular temperature, a near stoichiometric amount of TOPTe is injected. The growth temperature can be maintained for a few minutes to hours, leading to slow growth of the particles. Temperatures between 70°C and 120°C allow to reach a range of sizes such that the band edge covers the range from 2 microns to 8 microns at room temperature. An optimized procedure can lead to materials with multiple absorption features as seen Figure 3e. This is indicative of a good size dispersion reported at ≈ 5%. However, as seen in Figure 3d, the particles are not spherical and do not

appear particularly uniform in the TEM image, showing the possibility of further improvements.

Using cation exchange, it is possible to start from CdTe and CdSe nanoplatelets [23-25] (NPL) with a perfectly controlled thickness to generate NPL of HgTe and HgSe [26] shown in Figure 3g. These HgTe NPL present the advantages of the 2D geometry already observed for the cadmium chalcogenide compounds: (i) narrow optical feature (PL linewidth is below 60meV for an emission at 1.4eV) and fast emission (50ns PL lifetime). The optical absorption edge remains currently in the near infrared (800-1000nm), which correspond to 1.5eV of confinement energy, due to the small thickness of the NPL. The growth of thicker mercury chalcogenides NPL with sharp optical absorption in the mid-infrared has not yet reported.

B. Intraband transitions with HgS and HgSe CQDs

The intraband transition between the first two quantum confined states of CQDs is also an IR transition and many experiments explored the transition between the lowest conduction band states $1S_e$ to the next $1P_e$ state. While the infrared $1S_e$-$1P_e$ intraband absorption was observed in CdSe CQDs upon photoexcitation of carriers [27] or after charge transfer doping [28,29] the carriers were only stable in inert conditions. HgS [30] and HgSe [31,32] CQDs were found to be naturally n-doped and to show the infrared $1S_e$-$1P_e$ intraband absorption stable in ambient conditions.

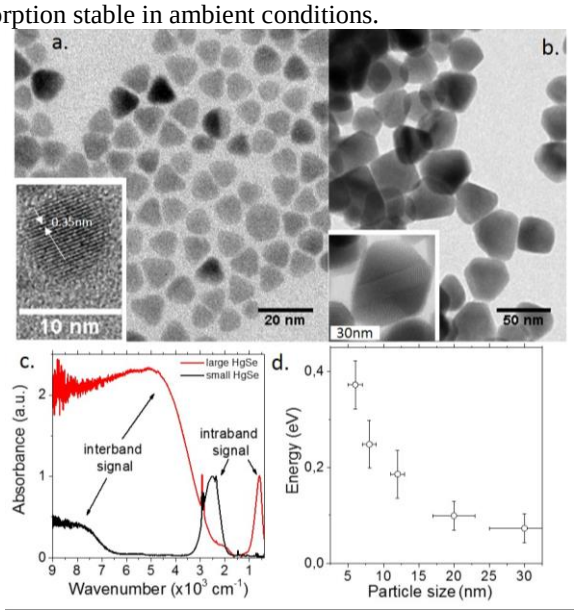

Figure 4 a. TEM image of small HgSe CQD. The inset is a high resolution image highlighting the lattice fringes. b.TEM image of large HgSe CQD. The inset is a high resolution image which show the polycristaline nature of the largest CQD. c absorption spectra of two sizes of HgSe CQD. The absorption arises from interband transitions at high energy and intraband transitions at low energy. Adapted from ref [32]. d Energy of the HgSe intraband absorption peak as a function of the nanoparticle size (diameter).The error bars represent the full width at half maximum of the size distribution obtained by TEM and the full width half maximum of the absorption peak.

*Figure 4*c show spectra of HgSe nanocrystals. At high energy the absorption is due to interband absorption. At smaller energy, there is the intraband absorption. As discussed further below, the relative intensity of the intraband absorption and interband excitonic absorption can be tuned by the surface chemistry. When extended to larger sizes as shown in Fig. 3b, the intraband absorption can be tuned to 20 microns [32]. HgS CQDs show similar optical properties. The zinc blend HgS is often reported as a zero-gap semiconductor in contrast to the more stable form of the red cinnabar which has a gap in the visible range, however CQD spectroscopy indicates that zinc blend HgS has a moderate gap of 0.65 eV [33].

The synthesis of HgS and HgSe CQDs derives from that of HgTe. TOPS and TOPSe being less reactive than TOPTe, seleneourea and thiourea have been used as sources of selenide and sulfide respectively. Another synthetic scheme used a more reactive mercury salt based on mercury acetate, in oleic acid and oleylamine, which allows reaction with TOPSe. This led to CQD with size below 15nm, see Figure 4a. Phosphine binds to Mercury and in an effort to obtain larger CQD, a phosphine free synthesis was developed [34]. With SeS_2 as a selenium precursor, larger (up to 50nm) HgSe CQD were reported [32], see Figure 4b.

Concerning the origin of doping in these two materials, the following points have been identified. (*i*) The doping is affected by surface modifications, see *Figure 5*a. Changing the ligand can significantly affect the $1S_e$ state occupation, see *Figure 5*b. Similarly the exposure to metal ions adsorption raises the doping level, while sulfide ions lower the doping level, see *Figure 5*c. (*ii*) The ratio of the intraband absorption and interband absorption [35] is shown for several different ligand exchanges in *Figure 5*a. (*iii*) The doping of the larger CQDs is far less affected by sulfides or ligand exchange than for small CQDs. (*iv*) For the larger CQD, the intraband signal gets narrower in spite of a worse size dispersion.

The stable doping of HgS and HgSe CQDs in ambient conditions constrains the energy of the $1S_e$ state to be close to the ambient Fermi level. The latter is between the reduction of H^+ to H_2, (-4.1 V vs vacuum at pH 7) and the reduction of water to oxygen (-5.3V vs vacuum at pH 7). This is made a priori possible by the large workfunction of the HgX CQD [36] and their narrow bad gap.

The surface sensitivity of the doping has been attributed to the energy shift of the CQD states due to a change of the electrostatic potential of the CQDs, relative to the ambient Fermi level [30]. A proposed mechanism is changes of the dipole moments at the surface. This is similar to work-function changes of metal surfaces due to the dipole layer set by adsorbates, and with organic monolayers of different dipole moment [37]. Adding a dipole layer shifts the energy of the states with respect to the Fermi level of the environment, according to $\Delta\phi = \sigma_d/\varepsilon_r\varepsilon_0$ where σ_d is the surface dipole density, ε_0 the vacuum permittivity and ε_r the medium dielectric constant. In narrow band gap materials, large effects can be expected with reasonable dipole magnitude. There have been several other studies on the suggested role of the dipole moment on CQD surfaces in adjusting the redox potentials [38] or in optimizing the injection barriers from dots to polymers [39]. However, direct measurements of the Fermi level and the dipole density have not yet been performed, and several prior studies reported no correlation between the dipole moment of the adsorbates and the energy level shifts of CQDs [40,41]. Complex effects have been observed with HgSe/CdS (see

*Figure 5*d) and HgS/CdS CQDs where the growth of a CdS shell can lead to a disappearance of the doping in a colloidal solution but recover in films. This indicates that doping is rather sensitive to the environment, which is both a challenge and an opportunity.

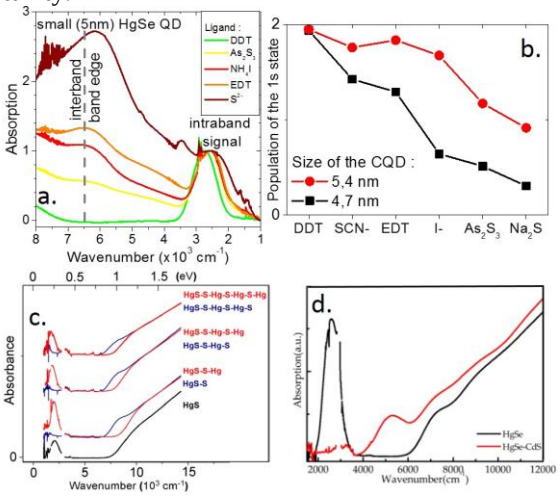

Figure 5a. Absorption spectra of small HgSe (5nm) CQD before and after their surface modification with the indicated ligands. b. Relative population of the conduction band $1S_e$ state for 4.7 and 5.7 nm HgSe CQD for different capping ligands, adapted from ref [35] c. Absorption spectra of HgS core upon successive exposures to S^{2-} and Hg^{2+} ions, adapted from ref 30. d. Absorption spectra of HgSe core and HgSe/CdS core shell CQD, adapted from ref. [42].

As the nanoparticles are made smaller, doping should be more difficult since electrons in the 1Se state may become too reducing for the environment, including the surface. Conversely, as the nanoparticles are grown larger, the higher energy quantum states may move below the environment Fermi level and pick up electrons. Therefore many more carriers may be present in the larger nanoparticle. At some point the intraband resonances of all the electrons may be better described as a collective surface plasmon resonance and this has been discussed for n-ZnO [43] and n-HgS [33].

C. Surfaces plasmons in semiconductor nanoparticles

While the connection between the intraband transitions and the surface plasmons is recent, surface plasmon resonances in semiconductor nanoparticles have been previously reported for several systems starting with $Cu_{2-x}S$ [44].The surface plasmon resonance arises from the free carriers of the material. It appears as an intense infrared absorption at energies below the semiconductor gap, just like an intraband transition. Other materials showing the surface plasmon resonance include Al: ZnO [45], In:CdO [46], P:Si [47] and several other systems. The reader is referred to recent reviews [48-50]. The surface plasmon resonance can be quite narrow. For example, In:CdO nanocrystals show a resonance as narrow as $\approx 700 cm^{-1}$ in the mid-IR [46]. Recent single particle linewidth for Al:ZnO nanocrystals have been measured to be $\approx 600\ cm^{-1}$ for a center position of $\approx 2500\ cm^{-1}$ [51]. Even narrower ensemble linewidth of $300\ cm^{-1}$ at a center position of $1000\ cm^{-1}$ have been observed for the larger HgS nanocrystals that are proposed to be highly doped and for which the resonance is also assigned to a plasmon [34]. While single electron intraband transitions narrow to meV widths at low temperatures [52], the plasmonic linewidths of doped nanocrystals are expected to remain broad even at low temperature because they are limited by carrier-carrier scattering. The fluorescence should also be very weak and it has not yet been reported for the semiconductor plasmonic nanoparticles. The carrier-impurity scattering rate can be minimized by using dopants with low scattering potentials and this can be extracted from the bulk effective mass and mobility. Using remote doping or charge transfer may also improve the linewidth. Narrower linewidths have indeed been observed with ITO nanoparticles with Sn segregated near the surface [53].

The evolution from the few electrons (intraband) to the many electrons (surface plasmon) has been discussed for metal nanoparticles [54-56] as well as for charge-transfer doped ZnO and HgS nanoparticles. The intraband-surface plasmon evolution is likely a rather generic feature of all nanoparticle semiconductors that can sustain many electrons. In the case of larger (10 nm) HgSe [32] and Ag_2Se nanoparticles [57], strong resonances in the LWIR were observed and assigned to quantum confinement but they may have a plasmonic character as well. The strong IR resonance afforded by the surface plasmon resonance of semiconductor nanoparticles could become beneficial for bolometric detection with narrow spectral response and it could be used to improve the optical properties of mid-IR devices.

III. Optical and Electrical Properties of HgTe, HgSe and HgS

For photodetection, the quantum efficiency of photocarrier generation and the lifetime of the carriers are important parameters. High efficiency requires that the photogenerated exciton rapidly dissociate and that the charge carriers travel to the collecting electrode without recombination. This calls for maximizing the mobility of the charge carriers and minimizing non-radiative recombination.

Eliminating non-radiative process is particularly challenging for small gap excitations. At present the mid-IR photoluminescence of CQDs is rather weak. For 2µm emission the PL efficiency is around 1% and drops to 0.01% at 5µm [58]. One difficulty is the presence of organic ligands on the CQD surface. The latter are typically made of organic molecules which also absorb in the mid-IR and the near field coupling of the semiconductor with the surrounding organic shell leads to fast energy transfer [59]. An example is shown in Figure 6a where the PL efficiency drops significantly as it overlaps with the C-H stretch vibration. A strategy is therefore to push the integration of the CQD into a fully inorganic matrix to prevent the charge transfer to the ligands [60].

The interband absorption of HgTe redshifts as the temperature decrease [61], see Figure 6a, of the order of $200\text{-}400 \mu eV.K^{-1}$ depending of the CQD size. MCT alloys show similar red shifts with decreasing temperature. The temperature dependence of the intraband transitions in HgSe is however opposite [31] and this is not yet explained.

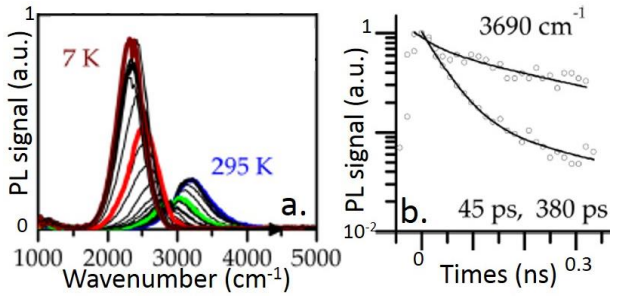

Figure 6 a. PL of HgTe CQD at different temperatures ranging from 300K to 7K. As the PL peak overlaps the C-H bond absorption, the PL efficiency drops, adapted from ref [58]. Time resolved photoluminescence for HgTe CQD. The PL lifetime presents two component, one around 50ps due to Auger recombination at higher pump power (lower curve), and one around 400ps due to non-radiative geminate recombination, adapted from ref [58].

The dynamic of carriers in narrow band gap CQDs materials has not yet been much investigated mostly due to technical limitations. An important issue with bulk IR detector materials is Auger recombination. Auger leads to short carrier lifetimes at room temperature and this strongly decreases the detectivity. With quantum dots there is a possibility of reduced Auger rates which would allow higher operation temperature. There are limited measurements of the Auger rate in HgTe CQDs and the biexciton Auger recombination is as fast as ≈ 50 ps. [58, 62], see *Figure 6*b. The narrow band gap of the HgX CQD have also attracted some attention for multiexciton generation [63] in HgTe [64] and HgCdTe [65] CQD. Obviously more needs to be done in this direction in the future.

As synthesized, the HgTe nanocrystals are rather intrinsic semiconductors [66,67] and films exhibit ambipolar character with similar electron and hole mobility, see *Figure 7*a-b, and this is a good feature for fast photodetection. Devices can be made in air and show good enough stability at the present stage of the development. The measured mobility depends on the nanocrystal synthesis procedure, likely by the difference in aggregation, and it may depend on the measurement method, using either electrochemical gating or solid state gating. Ligand exchange of the more dispersed HgTe CQD [22] with short organic ligand (such as ethanedithiol=EDT) leads to electrochemically measured ambipolar mobility of ~10^{-2} $cm^2V^{-1}s^{-1}$ [67] Values of 10^{-4}-10^{-3} $cm^2V^{-1}s^{-1}$ are reported when the same procedure is applied to HgSe nanocrystal [31].

Using an organic ligand may reduce the photocurrent efficiency and the ideal capping matrix needs to combine a low absorption in the mid infrared and a type I band alignment with the nanocrystal. Some success was reported with As_2S_3/propylamine as capping agent [68,69]. With HgTe CDQ this raised the carrier mobility compared to EDT [69] as shown in Fig.7b. In the case of HgSe, a mobility of 90 $cm^2V^{-1}s^{-1}$ has been reported [32] using a liquid phase ligand exchange with As_2S_3 derived ligands. While HgTe is ambipolar, HgSe and HgS show only n type behavior in different gating configurations, see *Figure 7*a-b. This is consistent with their n-doped character probed by optical measurements, see Figure 4c, and it may also indicate a lack of chemical stability as p-type materials. The presence of doping has been confirmed even at the single particle level using on chip tunnel spectroscopy [70].

The doping of the $1S_e$ followed by the $1P_e$ state has been reported by electrochemical gating with a reference electrode, see Figure 6c. The conductance displays a local minimum resulting from Pauli blockade once the $1S_e$ states is filled. The higher mobility from the $1P_e$ state as well as near quantitative 3-fold increase in electron loading was also reported. The transfer curve measured in a one electrode ion-gel gating, see Figure 6d, also display a non-monotonous gating that arises from filling the $1S_e$ state.

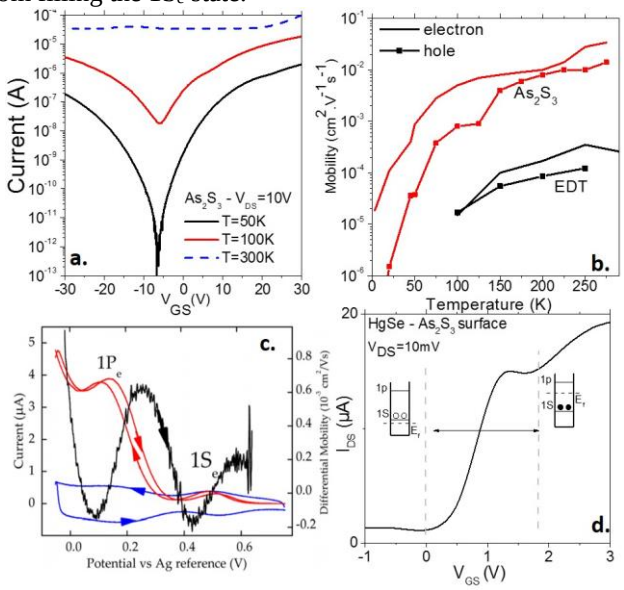

Figure 7 a Transfer curve (drain current vs gate voltage) for a field effect transistor with a channel made of HgTe CQD capped with As_2S_3 ligands. b mobility as a function of temperature for HgTe CQD with As_2S_3 or EDT, adapted from ref [69] c. Electrochemical gating of HgSe CQDs cross-linked with ethanedithiol, showing the electrochemical current (blue line), the conductance (red line), and the extracted differential mobility black curve. The peaks are assigned to the $1S_e$ and $1P_e$ states. d. Transfer curve of a electrolytic transistor with a made of HgSe CQD capped with As_2S_3 ligands., adapted from ref [32]. The curve presents a minimum, assigned to filling of the $1S_e$ state.

IV. Photodetection properties of HgTe, HgSe and HgS

Photoconduction with HgTe nanocrystal was first investigated [71] in the near-infrared for the telecom wavelengths [20,72,73] and for solar cell [74,75]. Mid-infrared photoconduction is at present the property of the HgX CQD which drives the most interest in these materials [76,77].

In the mid-infrared, HgX devices have been operated in a photoconductive and photovoltaic geometry [78]. Photoconductive devices are built by drop-casting materials on (interdigitated) electrodes. In terms of performance, a limitation is that complete light absorption requires rather thick films. Another limitation is the *1/f* noise [79] that is present in biased systems. As shown in *Figure 1*, the specific detectivity is a traditional measure of performance, and various reported values of the D* of HgX CQDs are indicated. For better comparisons, one would also need to report the response temporal bandwidth as this allows to distinguish between bolometers and quantum detectors operation. The best HgTe CQD detector properties reported to date at 5 microns are with the photovoltaic geometry, see *Figure 8*a. With this geometry, and with 0V bias, the detectivity was reported to be in the regime of Background

Limited Infrared Performance (BLIP) where the noise is limited by the 295K background radiation [78], along with response times of microseconds, internal quantum efficiency of 40%, and specific detectivity of $4x10^{10}$ Jones at 5 microns.

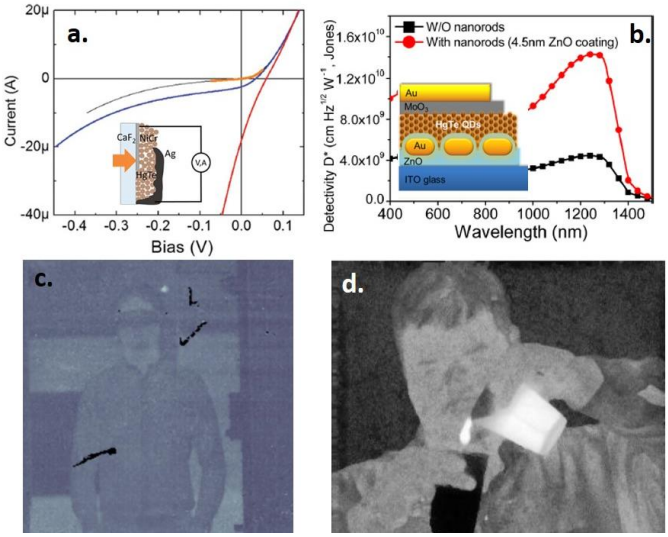

Figure 8 a. Current as a function of applied bias for a photovoltaic device at 90K in the dark condition (black line), receiving ambient 295K radiation (blue line) and receiving 600ºC blackbody illumination (red line). A scheme of the device is given as inset, adapted from ref [78]. b. Spectral dependence of the detectivity of a HgTe CQD film coupled or not to a plasmonic structure, adapted from ref [82]. c. and d. are images of a focal plane array for which the active layer is HgTe CQD, adapted from refs [80,81].

At present, the detectivity of CQDs decreases very fast with increasing temperature or for redder wavelengths. The reddest detection with HgTe dots has been demonstrated up to 12 microns but with low detectivity of ≈ 10^7 Jones at 80K. When dealing with the design of infrared detector material, the final judge remains the formation of an image. By coupling a film of HgTe CQD with a silicon read out circuit, the first mid-IR imaging with CQD was recently reported [80].*Figure 8*c-d shows an image taken at 120 frame per second to illustrate the faster response than bolometer cameras. The reported noise equivalent temperature difference (NETD) was 100mK for 5 microns imaging [81].

The mid-IR CQDs need significant improvements before they can become a viable competition to existing technologies. One advantage of solution processing is that it affords device improvement strategies which may not be as easily applied to the wafer materials. By coupling near-IR HgTe CQD with gold nanorods, Chen *et al* [82] reported a three-fold improvement in detectivity shown in *Figure 8*b. Coupling the absorption of the MWIR CQD with plasmonic structures [83, 84] allows to increase the absorption of thin layers of CQDs. The pixel formation of Visible/mid-IR bicolor [85] and MWIR Multispectral detectors is also be facilitated with solution processing [86]. Finally, there is a need to develop less toxic materials. Even if the CQDs lead to cheap and performant cameras, the toxicity of Hg is a serious concern for consumer electronics. Possible alternatives such as Cd_3As_2 and PbSnTe should be investigated. The intraband approach should allow a much wider range of materials. Although CQD intraband photodetection has barely started to be investigated, there is also the possibility of fundamental advantages such as better control of Auger process and narrower spectral detection.

V. CONCLUSION

Over the past few years, HgTe CQDs have been the leading materials for CQD based MWIR photodetection, having demonstrated BLIP performance, fast response and integration into camera imaging. The introduction of self-doped nanocrystals of HgSe and HgS has also allowed to use intraband transitions as an alternative route to mid-IR CQD detectors. With these initial demonstrations of some degree of feasibility within a relatively short time, one may expect a significant growth in this field.

The research is partly driven by the end-goal of performant and affordable uncooled infrared imaging. There are many possible directions to follow in order to address the numerous challenges. Higher mobility and longer carrier lifetimes need to be achieved, possibly by inorganic encapsulation. As in bulk materials, small changes of doping have large effects on device performances and doping needs to become a controllable property. Optical management, using various methods, from dielectric stacks to plasmonics, will need to be investigated to maximize the photon collection efficiency. There is a need and an opportunity to develop new nanofabrication process which preserve or enhance the CQD properties. Developing lower toxicity compounds will be crucial for consumer electronic applications and there will be a need to achieve long term stability in devices. With such progress, CQDs could indeed transform IR technologies.

REFERENCES

[1] H. Schneider and H.C. Liu, Quantum well infrared photodetectors, Physics and applications (Springer, Heidelberg, 2006).

[2] K. W Berryman, S. A. Lyon and M. Segev, " Mid-infrared photoconductivity in InAs quantum dots" *Appl. Phys. Lett*. vol. 70, pp. 1861-1863, 1997.

[3] D. Pan, E. Towe and S. Kennerly , "Normal-incidence intersubband (In, Ga)As/GaAs quantum dot infrared photodetectors", *Appl. Phys. Lett*. vol. 73, pp. 1937-1939, 1998.

[4] S. Sauvage, P. Boucaud, T. Brunhes, V. Immer, E. Finkman and J. M. Gerard, "Midinfrared absorption and photocurrent spectroscopy of InAs/GaAs self-assembled quantum dots" *Appl. Phys. Lett.* vol. 78, pp. 2327-2329, 2001

[5] S. Chakrabarti, A D. Stiff-Roberts, X.H. Su, P. Bhattacharya, G. Ariyawansa and A.G.U..; Perera, "High-performance mid-infrared quantum dot infrared photodetectors", *J. Phys. D, Appl. Phys.* vol. 38, pp. 2135-2141, 2005.

[6] H. Lim, S. Tsao, W. Zhang and M. Razeghi "High-performance quantum-dot infrared photodetectors grown on InP substrate operating at room temperature", *Appl. Phys. Lett*. vol. 90, pp. 131112, 2007.

[7] P. Martyniuk and A Rogalski, "Quantum-dot infrared photodetectors: Status and outlook", *Prog. Quantum Elec. vol.* 32, pp. 89-120, 2008

[8] E. Rosencher and B. Vinter, « Optoélectronique », 2nd ed. Dunod, Paris, 2002.

[9] J. S. Steckel, J. Ho, C. Hamilton, J. Xi, C. Breen, W. Liu, P. Allen and S. Coe-Sullivan "Quantum dots: The ultimate down-conversion material for LCD displays", J. *Soc. Inf. Disp*. vol. 23, pp. 294-305, 2015.

[10] S. V. Kershaw, A. S. Susha and A. L. Rogach, "Narrow bandgap colloidal metal chalcogenide quantum dots: synthetic methods, heterostructures, assemblies, electronic and infrared optical properties," *Chem. Soc. Rev*. vol. 42, pp. 3033, 2013.

[11] S. V. Kershaw, A. L. Rogach. Infrared Emitting HgTe "Quantum Dots and their Waveguide and Optoelectronic Devices". *Z. Phys. Chem.* vol. 229, pp.23-64, 2015.
[12] E. Lhuillier, S. Keuleyan, H Liu and P. Guyot-Sionnest, "HgTe quantum dot for mid IR application," *Chem. Mat* vol. 25, pp. 1272, 2013.
[13] S. E. Keuleyan, P. Guyot-Sionnest, C. Delerue, and G. Allan, "Mercury Telluride Colloidal Quantum Dots: Electronic Structure, Size-Dependent Spectra, and Photocurrent Detection up to 12 μm" *ACS Nano* vol. 8, pp. 8676-8682, 2014.
[14] G. Allan and Christophe Delerue, "Tight-binding calculations of the optical properties of HgTe nanocrystals," *Phys. Rev. B* vol. 86, pp. 165437, 2012.
[15] A.L. Rogach, A. Eychmuller, S.G. Hickey and S.V. Kershaw, "Infrared-emitting colloidal nanocrystals: Synthesis, assembly, spectroscopy, and applications," *Small* vol. 3, pp. 536–557, 2007.
[16] D. Schooss, A. Mews, A. Eychmüller and H. Weller, "Quantum-dot quantum well CdS/HgS/CdS: Theory and experiment" *Physical Review B* vol. 49, no 24, pp. 17072, 1994.
[17] A. Rogach, S. Kershaw, M. Burt, M. Harrison, A. Kornowski, A. Eychmuller and H. Weller, "Colloidally Prepared HgTe Nanocrystals with Strong Room-Temperature Infrared Luminescence" *Adv. Mater*. vol. 11, pp.552–555, 1999.
[18] M. Kuno, K.A. Higginson, S.B. Qadri, M. Yousuf, S. H. Lee, B.L. Davis and H. Mattoussi, "Molecular clusters of binary and ternary mercury chalcogenides: colloidal synthesis, characterization, and optical spectra" *J. Phys. Chem. B* vol. 107, pp. 5758–5767, 2003.
[19] P. Howes, M. Green, C. Johnston and A. Crossley, "Synthesis and shape control of mercury selenide (HgSe) quantum dots" *J. Mater. Chem*. vol. 18, pp. 3474–3480, 2008.
[20] M.V. Kovalenko, E. Kaufmann, D. Pachinger, J. Roither, M. Huber, J. Stangl, G. Hesser, F. Schaffler and W. Heiss, "Colloidal HgTe nanocrystals with widely tunable narrow band gap energies: from telecommunications to molecular vibrations" *J. Am. Chem. Soc.* vol. 128, pp. 3516–3517, 2008.
[21] S. Keuleyan, E. Lhuillier, V. Brajuskovic and P. Guyot-Sionnest, "Mid-infrared HgTe colloidal quantum dot photodetectors" *Nat Photon. vol.* 5, pp.489-493, 2011.
[22] S. Keuleyan, E. Lhuillier and P. Guyot-Sionnest, "Synthesis of Colloidal HgTe Quantum Dots for Narrow Mid-IR Emission and Detection" *J. Am. Chem. Soc.* vol. 133, pp. 16422-16424, 2011.
[23] J. Joo, J. S. Son, S. G. Kwon, J. H. Yu and T. Hyeon, "Low-Temperature Solution-Phase Synthesis of Quantum Well Structured CdSe Nanoribbons" J. *Am. Chem. Soc*. vol. 128, pp. 5632−5633, 2006.
[24] M. Nasilowski, B. Mahler, E. Lhuillier, S. Ithurria and B. Dubertret, "2D Colloidal nanocrystals" *Chem Rev*. vol. 116, pp 10934−10982, 2016.
[25] E. Lhuillier, S. Pedetti, S. Ithurria, B. Nadal, H. Heuclin and B. Dubertret, "2D Colloidal Metal Chalcogenides Semiconductors: Synthesis, Spectroscopy and Applications " *Acc. Chem. Res.* Vol. 22, pp 48, 2015.
[26] E. Izquierdo, A. Robin, S. Keuleyan, N. Lequeux, E. Lhuillier and S. Ithurria, "Strongly confined HgTe 2D nanoplatelets as narrow near infrared emitter" J. *Am. Chem. Soc.* vol. 138, pp 10496–10501, 2016.
[27] K. S. Jeong and P. Guyot-Sionnest, "Mid-Infrared Photoluminescence of CdS and CdSe Colloidal Quantum Dots," *ACS Nano* vol. 10, pp. 2225−2231, 2016.
[28] M. Shim and P. Guyot-Sionnest, "N-type colloidal semiconductor nanocrystals," *Nature* vol. 407, pp. 981-983, 2000.
[29] C. Wang, M. Shim, P. Guyot-Sionnest, "Electrochromic nanocrystal quantum dots" *Science* vol. 291, pp. 2390-2392, 2001.
[30] K. S. Jeong, Z. Deng, S. Keuleyan, H. Liu and P. Guyot-Sionnest, "Air-Stable n-Doped Colloidal HgS Quantum Dots" *J. Phys. Chem. Lett.* Vol. 5, pp.1139−1143, 2014.
[31] Z. Deng, K. Seob Jeong and P. Guyot-Sionnest , "Colloidal Quantum Dots Intraband Photodetectors," *ACS Nano* vol. 8, pp. 11707-11714, 2014.
[32] E. Lhuillier, M. Scarafagio, P. Hease, B. Nadal, H. Aubin, X. Z. Xu, N. Lequeux, G. Patriache, S. Ithurria and B. Dubertret, "Infrared photo-detection based on colloidal quantum-dot films with high mobility and optical absorption up to the THz" *Nano Lett* vol. 16, pp 1282-1286, 2016.
[33] G. Shen and P. Guyot-Sionnest, "HgS and HgS/CdS Colloidal Quantum Dots with Infrared Intraband Transitions and Emergence of a Surface Plasmon," *J. Phys. Chem. C* vol. 120, pp. 11744−11753, 2016.
[34] H. Mirzai, M. N. Nordin, R. J. Curry, J.-S. Bouillard, A. V. Zayats and M. Green "The room temperature phosphine-free synthesis of near-infrared emitting HgSe quantum dots" *J. Mater. Chem. C*, vol. 2, pp. 2107, 2014
[35] A. Robin, C. Livache, S. Ithurria, E. Lacaze, B. Dubertret and E. Lhuillier, "Surface Control of Doping in self-doped Nanocrystals" *ACS Appl. Mat. Interface* vol. 8, pp 27122–27128, 2016.
[36] A. H. Nethercot, Jr. "Prediction of Fermi Energies and Photoelectric Thresholds Based on Electronegativity Concepts " Phys. Rev. Lett vol.33, pp. 1088, 1974
[37] I. H. Campbell, S. Rubin, T.A. Zawodzinski, J.D. Kress, R. L. Martin, D. L. Smith, N.N. Barashkov and J.P. Ferraris, "Controlling Schottky Energy Barriers in Organic Electronic Devices using Self-assembled Monolayers". *Phys. Rev. B* vol. 54, pp.14321-14324, 1996.
[38] G. M. Carroll, E.Y. Tsui, C.K. Brozek and D.R. Gamelin, "Spectroelectrochemical Measurement of Surface Electrostatic Contributions to Colloidal CdSe Nanocrystal Redox Potentials" Chem. Mat. vol. 28, pp. 7912–7918, 2016
[39] C. H. M. Chuang, P.R. Brown, V. Bulovic and M.G. Bawendi, "Improved performance and stability in quantum dot solar cells through band alignment engineering", *Nature Mat.* vol. 13, pp.796-801, 2014.
[40] M. Soren-Harini, N. Yaacobi-Gross, D. Stenin, A. Aharoni, U. Banin, O. Milo and N. Tessler, "Tuning energetic levels in nanocrystal quantum dots through surface manipulations", *Nano Lett.* vol. 8, pp. 678-684, 2008.
[41] J. Jaseniak, M. Califano and S.E. Watkins, "Size-dependent valence and conduction band edge energies of semiconductor nanocrystals", *ACS Nano* vol. 5, pp.5888-5902, 2011.
[42] Z. Deng and P. Guyot-Sionnest, "Intraband Luminescence from HgSe/CdS Core/Shell Quantum Dots", *ACS Nano* vol. 10, pp. 2121-2127, 2016.
[43] A.M. Schimpf, N. Thakkar, C.E. Gunthardt, D.J. Masiello and D.R. Gamelin, "Charge-Tunable Quantum Plasmons in Colloidal Semiconductor Nanocrystals" *ACS Nano* vol. *8*, pp. 1065-1072, 2014.
[44] Y. Zhao, H. Pan, Y. Lou, X. Qiu, J. Zhu and C. Burda, «Plasmonic Cu2-xS Nanocrystals: Optical and Structural Properties of Copper-deficient Copper (I) Sulfides" *J. Am. Chem. Soc*., vol. 131, pp.4253-4261, 2009.
[45] R. Buonsanti, A. Llordes, S. Aloni, B.A. Helms and D.J. Milliron, " Tunable Infrared Absorption and Visible Transparency of Colloidal Aluminum-doped Zinc Oxide Nanocrystals". *Nano Lett.* vol. 11, pp. 4706-4710, 2011.
[46] T.R. Gordon, T. Paik, D.R. Klein, G.V. Naik, H. Caglayan, A. Boltasseva and C.B. Murray, "Shape-Dependent Plasmonic Response and Directed Self-Assembly in a New Semiconductor Building Block, Indium-Doped Cadmium Oxide (ICO)" *Nano Lett.* vol. 13, pp.2857− 2863, 2013.
[47] D.J. Rowe, J.S. Jeong, A. Mkhoyan and U.R. Kortshagen, "Phosphorus-Doped Silicon Nanocrystals Exhibiting Mid-Infrared Localized Surface Plasmon Resonance" *Nano Lett*. vol. 13, pp 1317-1322, 2013.
[48] X. Liu and M.T. Swihart, " Heavily-doped colloidal semiconductor and metal oxide nanocrystals: an emerging new class of plasmonic nanomaterials" *Chem. Soc. Rev*. vol.43, pp. 3908-3920, 2014.
[49] F. Scotognella, G. D. Valle, A.R.S. Kandada, M. Zavelani-Rossi, A. Comin, S. Longhi, L. Manna, G. Lanzani and F. Tassone, "Plasmonics in Heavily-doped Semiconductor Nanocrystals" *Eur. Phys. J. B*, vol. 86, pp.154, 2013.
[50] S. D. Lounis, E. L. Runnerstrom, A Llordés and D. J. Milliron, "Defect Chemistry and Plasmon Physics of Colloidal Metal Oxide Nanocrystals" J. *Phys. Chem. Lett*. vol. 5, pp.1564–1574, 2014.
[51] R.W. Johns, H.A. Bechtel, E.L. Runnerstrom, A. Agrawal, S.D. Lounis, D.J. Milliron, Direct observation of narrow mid-infrared plasmon linewidths of single metal oxide nanocrystals, *Nature Comm*. vol. 7, pp 11583, 2016
[52] M. Shim and P. Guyot-Sionnest, "Intraband hole burning of colloidal quantum dots", *Phys. Rev*. B vol. 64, pp. 245342, 2001.
[53] S. D. Lounis, E. L. Runnerstrom, A. Bergerud, D. Nordlund, D. J. Milliron Influence of Dopant Distribution on the Plasmonic Properties of Indium Tin Oxide Nanocrystals, *J. Am. Chem. Soc*. vol. *136*, pp 7110–7116, 2014.
[54] L. Genzel, T.P. Martin and U. Kreibig, "Dielectric Function and Plasma Resonances of Small Metal Particles" *Zeitschrift für Physik B Condensed Matter* vol. *21*, pp. 339-346, 1975.
[55] P.K. Jain, " Plasmon-in-a-Box: On the Physical Nature of Few-Carrier Plasmon Resonances" J. *Phys. Chem. Lett*. vol. *5*, pp. 3112-3119, 2014.
[56] H. Zhang, V. Kulkarni, E. Prodan, P. Nordlander and A.O. Govorov, " Theory of Quantum Plasmon Resonances in Doped Semiconductor Nanocrystals" J. *Phys. Chem C* vol. *118*, pp.16035-16042, 2014.
[57] A. Sahu, A. Khare, D. D. Deng and D. J. Norris, "Quantum confinement in silver selenide semiconductor nanocrystals," *Chem. Commun*. vol.48, pp.5458–5460, 2012.
[58] S. Keuleyan, J. Kohler and P. Guyot-Sionnest, "Photoluminescence of Mid-Infrared HgTe Colloidal Quantum Dots" *J. Phys. Chem. C* vol. 118, pp. 2749−2753, 2014.
[59] H. Liu and P. Guyot-Sionnest, "Photoluminescence Lifetime of Lead Selenide Colloidal Quantum Dots," *J. Phys. Chem. C* vol. 114, pp.14860-14863, 2010.

[60] M. V. Kovalenko, R. D. Schaller, D. Jarzab, M. A. Loi and D. V. Talapin. Inorganically Functionalized PbS–CdS Colloidal Nanocrystals: Integration into Amorphous Chalcogenide Glass and Luminescent Properties" *J. Am. Chem. Soc*. vol. 134, pp.2457–2460, 2012.

[61] E. Lhuillier, S. Keuleyan and P. Guyot-Sionnest, "Optical properties of HgTe colloidal quantum dots" *Nanotechnology* vol. 23, pp. 175705, 2012.

[62] A. Al-Otaify, S.V. Kershaw, S. Gupta, A.L. Rogach, G. Allan, C. Delerue, D.J. Binks, Multiple exciton generation and ultrafast exciton dynamics in HgTe colloidal quantum dots, *Phys. Chem. Chem. Phys*. vol.15, pp 16864-16873, 2013

[63] J. A. McGuire, J. Joo, J. M. Pietryga, R. D. Schaller and V. I. Klimov, "New Aspects of Carrier Multiplication in Semiconductor Nanocrystals," *Acc. Chem. Res*. Vol. 41, pp 1810–1819, 2008.

[64] A. Al-Otaify, S. V. Kershaw, S. Gupta, A. L. Rogach, G. Allan, C. Delerue and D.. J. Binks, "Multiple exciton generation and ultrafast exciton dynamics in HgTe colloidal quantum dots," *Phys. Chem. Chem. Phys*. vol.15, pp. 16864, 2013.

[65] S. V. Kershaw, S. Kalytchuk, O. Zhovtiuk, Q. Shen, T. Oshima, W. Yindeesuk, T. Toyodab and A. L. Rogach, "Multiple exciton generation in cluster-free alloy $Cd_xHg_{1-x}Te$ colloidal quantum dots synthesized in water," *Phys. Chem. Chem. Phys*. vol. 16, pp. 25710, 2014.

[66] E. Lhuillier, S. Keuleyan, P. Rekemeyer and P. Guyot-Sionnest, "Thermal properties of mid infrared Colloidal quantum dot detectors*" J. Appl. Phys* vol. 110, pp. 032110, 2011.

[67] H. Liu, S. Keuleyan, and P. Guyot-Sionnest, "n- and p-Type HgTe Quantum Dot Films," *J. Phys. Chem. C* vol. 116, pp. 1344–1349, 2012.

[68] S. Yakunin, D. N. Dirin, L. Protesescu, M. Sytnyk, S. Tollabimazraehno, M. Humer, F. Hackl, T. Fromherz, M. I. Bodnarchuk, M. V. Kovalenko, and W. Heiss "High Infrared Photoconductivity in Films of Arsenic-Sulfide-Encapsulated Lead-Sulfide Nanocrystals" *ACS Nano* vol. 8, pp. 12883–12894, 2014.

[69] E. Lhuillier, S. Keuleyan, P. Zolotavin and P. Guyot-Sionnest, "Mid-Infrared HgTe/As_2S_3 FETs and photodetectors," *Adv. Mat.* Vol. 25, pp. 137-141, 2013.

[70] H. Wang, E. Lhuillier, Q. Yu, A. Zimmers, B. Dubertret, C. Ulysse and H. Aubin, "Transport in a Single Self-Doped Nanocrystal", *ACS Nano* vol 11, pp 1222-1229 (2017).

[71] H. Seong, K. Cho and S. Kim "Photocurrent characteristics of solution-processed HgTe nanoparticle thin films under the illumination of 1.3 μm wavelength light" *Semi. Sci. Tech.* vol. 23, pp. 075011, 2008.

[72] M. K. Jana, P. Chithaiah, B. Murali, S. B. Krupanidhi, K. Biswas and C. N. R. Rao" Near infrared detectors based on HgSe and HgCdSe quantum dots generated at the liquid–liquid interface" *J. Mater. Chem. C* vol. 1,pp. 6184-6187, 2013.

[73] M. Chen , H. Yu , S. V. Kershaw , H. Xu , S. Gupta , F. Hetsch , A. L. Rogach and Ni Zhao "Fast, Air-Stable Infrared Photodetectors based on Spray-Deposited Aqueous HgTe Quantum Dots" , *Adv. Funct. Mater*. vol. 24, pp. 53–59, 2014.

[74] S. H. Im, H. Kim, S. W. Kim, S.-W. Kim and S. Il Seok, "Efficient HgTe colloidal quantum dot-sensitized near-infrared photovoltaic cells," *Nanoscale* vol. 4, pp.1581-1584, 2012.

[75] M. Nam, S. Kim, S. Kim, S. Jeong, S.-W. Kim and K. Lee, "Near-infrared-sensitive bulk heterojunction solar cells using nanostructured hybrid composites of HgTe quantum dots and a low-band gap polymer" *Solar Energy Materials & Solar Cells* vol. 126, pp. 163–169, 2014.

[76] E. Lhuillier, S. Keuleyan and P. Guyot-Sionnest, "Colloidal quantum dot for mid-IR applications*" Infrared Phys. Tech.* vol. 59, pp. 133, 2013

[77] E. Lhuillier, S. Keuleyan, H. Liu and P. Guyot-Sionnest, *"Colloidal HgTe material for low cost detection into the MWIR***"** *J. Elec. Mat* vol. 41, pp. 2725, 2012.

[78] P. Guyot-Sionnest and J. Andris Roberts, "Background limited mid-infrared photodetection with photovoltaic HgTe colloidal quantum dots," *Appl. Phys. Lett.* vol. 107, pp. 253104, 2015.

[79] H. Liu, E. Lhuillier, P. Guyot-Sionnest, 1/f Noise in Semiconductor and Metal Nanocrystal Solids", *J. Appl. Phys*. vol. 115, pp.154309, 2014.

[80] A. J. Ciani, R. E. Pimpinella, C. H. Grein and P. Guyot-Sionnest, "Colloidal Quantum Dots for Low-Cost MWIR Imaging" *Proc. of SPIE* Vol. 9819, pp. 981919, 2016.

[81] C. Buurma, R.E. Pimpinella, A. J. Ciani, J. S. Feldman, C. H. Grein and P. Guyot-Sionnest, "MWIR imaging with low cost colloidal quantum dot films", Proc. SPIE vol. 9933, pp. 993303, 2016.

[82] M. Chen, L. Shao, S. V. Kershaw, H. Yu, J. Wang, A. L. Rogach and Ni Zhao, "Photocurrent Enhancement of HgTe Quantum Dot Photodiodes by Plasmonic Gold Nanorod Structures," *ACS Nano* vol. 8, pp 8208–8216, 2014.

[83] X. Tang, G. F. Wu and K.W. Chiu Lai, "Plasmon resonance enhanced colloidal HgSe quantum dot filterless narrowband photodetectors for mid-wave infrared", *J. Mater. Chem. C*, vol. 5, pp.362-369, 2017.

[84] Y. Yifat, M. Ackerman and P. Guyot-Sionnest, "Mid-IR colloidal quantum dot detectors enhanced by optical nano-antennas", *Appl. Phys. Lett.* 110, 041106, 2017

[85] E. Lhuillier, A. Robin, S. Ithurria, H. Aubin and B. Dubertret, "Electrolyte gated colloidal nanoplatelets based phototransistor and its use for bicolor detection" *Nano Lett*. vol. 14, pp. 2715-2719, 2014.

[86] Xin Tang, Xiaobing Tang, and King Wai Chiu Lai , "Scalable Fabrication of Infrared Detectors with Multispectral Photoresponse Based on Patterned Colloidal Quantum Dot Films" *ACS Photonics*, 3, pp 2396-2404, 2016.

Emmanuel Lhuillier did his PhD at Onera under the supervision of Emmanuel Rosencher on the electronic transport of superlattices. In 2010, he joined the Guyot-Sionnest group, developing the photoconductive properties of HgTe nanocrystals. In 2012, he joined the Dubertret's group at ESPCI where he investigated the optoelectronic properties of colloidal quantum wells. Since 2015, he is a CNRS research scientist in the Institute of Nanoscience at Sorbonne university, his group is dedicated to the optoelectronic studies of confined materials.

Philippe Guyot-Sionnest is a graduate from Ecole Polytechnique, France, and obtained his physics PhD from UC Berkeley under the supervision of Yuen Ron Shen, on the topic of surface nonlinear optics. His research group at the University of Chicago started in 1991 and has contributed to CQD research since, including the core/shell strategy for improved fluorescence, charge transfer doping, conductivity, and the more recent mid-IR applications.